Psychopharmacology (2008) 201:1–13
DOI 10.1007/s00213-008-1236-2

ORIGINAL INVESTIGATION

# Individual contribution of metabotropic glutamate receptor (mGlu) 2 and 3 to c-Fos expression pattern evoked by mGlu2/3 antagonism

**Alfred Hetzenauer · Corrado Corti · Stefanie Herdy · Mauro Corsi · Francesco Ferraguti · Nicolas Singewald**

Received: 28 December 2007 / Accepted: 10 June 2008 / Published online: 24 September 2008


**Abstract**
*Objectives and materials and methods* The aims of the present study were (1) to determine the neuronal activation pattern elicited by the group II mGlu antagonist LY341495 and (2) to evaluate the contribution of each group II mGlu subtype by using wild-type (WT) and knockout (KO) mice lacking either mGlu2 or mGlu3. c-Fos expression was used as a marker of neuronal activation.
*Results and discussion* In WT mice, LY341495 induced widespread c-Fos expression in 68 out of 92 brain areas, including limbic areas such as the amygdala, septum, prefrontal cortex, and hippocampus. LY341495-induced c-Fos response was markedly decreased in the medial part of the central amygdala (CeM) and lateral septum (LS) in mGlu3-KO mice, as well as in the lateral parabrachial nucleus (LPB) in both KO strains. In the majority of investigated areas, LY341495-induced c-Fos expression was similar in KO and WT mice. Analysis of the cellular and subcellular distribution of mGlu2 and mGlu3 revealed a prevailing presence of mGlu3-immunoreactivity in the CeM in glial processes and in postsynapstic neuronal elements, whereas only rare presynaptic axon terminals were found immunoreactive for mGlu2.
*Conclusion* In conclusion, our data indicate that group II mGlu blockade increases neuronal activation in a variety of brain areas, including many stress- and anxiety-related areas. The activation of two key brain areas, the CeM and LS, is mediated via mGlu3, while activation in the LPB involves both subtypes. Moreover, in the majority of investigated areas, LY341495-mediated neuronal activation appears to require a complex cross talk between group II mGlu subtypes or the action of LY341495 on additional receptors.

**Keywords** Metabotropic glutamate receptors · Neuronal activation · c-Fos · Amygdala · Lateral septum · LY341495 · Stress · Anxiety

A. Hetzenauer · S. Herdy · N. Singewald (✉)
Department of Pharmacology and Toxicology,
Institute of Pharmacy and Center for Molecular Biosciences Innsbruck (CMBI), University of Innsbruck,
Peter-Mayer-Str. 1,
A-6020 Innsbruck, Austria
e-mail: nicolas.singewald@uibk.ac.at

C. Corti · M. Corsi
Department of Biology, Psychiatry Centre of Excellence in Drug Discovery, GlaxoSmithKline Medicines Research Centre,
37135 Verona, Italy

F. Ferraguti
Department of Pharmacology, Innsbruck Medical University,
Innsbruck, Austria

## Introduction

Glutamate acts through ligand-gated ion channels and G protein-coupled metabotropic receptors (mGlus). At present, eight subtypes of mGlus receptors have been identified, which can be subdivided into three groups (group I: mGlu1, 5; group II: mGlu2, 3; group III: mGlu4, 6, 7, 8) based on their molecular structure, intracellular transduction pathway, and pharmacological profile (Conn and Pin 1997; Schoepp et al. 1999). Group II mGlu ligands seem to be drugs with a particular promising therapeutic potential in psychiatric disorders, including anxiety and depression (Johnson et al. 2005; Palucha and Pilc 2007). Group II

mGlus are widely expressed in the rodent forebrain, although the distribution of mGlu2 is more restricted than that of mGlu3 (Ferraguti and Shigemoto 2006). In neurons, mGlu2 and mGu3 receptors have been reported at both pre- and postsynaptic sites; however, their precise subcellular distribution has been investigated only in the hippocampal formation, striatum, and ventrobasal thalamus (Tamaru et al. 2001). mGlu3, but not mGlu2, receptors are also expressed in glial cells where they are negatively linked to adenylyl cyclase (Schoepp 2001). Activation of presynaptic mGlu2/3 has been reported to provide negative feedback regulation on the release of various neurotransmitters including glutamate, γ-aminobutyric acid (GABA), and dopamine (Cartmell and Schoepp 2000). On the other hand, postsynaptic mGlu2/3 receptors can negatively modulate neuronal excitability and plasticity upon stimulation (Anwyl 1999).

The recent development of drugs selective for group II mGlus, such as the agonist LY354740 (1S,2S,5R,6S)-2-aminobicyclo[3.1.0]hexane-2,6-dicarboxylic acid and the antagonist LY341495 [2*S*-2-amino-2-(1*S*,2*S*-2-carboxycyclo-prop-1-yl)-3-(xant-9-yl) propanoic acid] (Monn et al. 1997; Ornstein et al. 1998) has facilitated the elucidation of some of the physiological roles of these receptors. Activation of mGlu2 and mGlu3 by LY354740 elicits inhibitory responses and has frequently been reported to have anxiolytic-like properties in various anxiety-related tests, such as stress-induced hyperthermia and the elevated plus maze in wild-type (WT) mice (Helton et al. 1998; Linden et al. 2004; Linden et al. 2005a; Monn et al. 1997; Spooren et al. 2002; Johnson et al. 2005; Galici et al. 2006). Interestingly, recent studies involving mice lacking mGlu2 or mGlu3 receptors revealed that stimulation of both of these subtypes is necessary to observe anxiolytic-like efficacy of LY354740, since this effect was abolished in both knockout strains (Linden et al. 2005b). LY354740 (as prodrug) was also reported to be efficacious in the treatment of generalized anxiety disorders in humans (Dunayevich et al. 2008). Finally, a close analogue of LY354740, namely, LY404039, has been shown in a phase II clinical trial to improve both positive and negative symptoms in schizophrenia (Patil et al. 2007).

The important therapeutic implications that drugs acting at group II mGlus may have for anxiety and psychotic disorders, raise the question about the neural mechanisms involved in their therapeutic efficacy. It is hypothesized that the group II mGlu antagonist LY341495, by blocking inhibitory pre- and postsynaptic mechanisms, increases neuronal activation preferentially in anxiety-related brain areas. In order to test this hypothesis, we applied LY341495 to wild-type (WT) mice and evaluated c-Fos expression as a marker for neuronal activation (Hoffman and Lyo 2002). However, since LY341495 binds to both mGlu2 and mGlu3 receptors in a nanomolar range (Kingston et al. 1998; Ornstein et al. 1998), and no subtype-selective antagonists are currently available, it is difficult to evaluate the individual contribution of each group II mGlu receptor. In this respect, we have recently developed mGlu3-null mice, which have been instrumental for determining the specific role of mGlu3 in the LY354740 neuroprotective effect both in vitro and in vivo (Corti et al. 2007). Hence, we decided to use knockout (KO) mice lacking either mGlu2 or mGlu3 receptors to examine their individual contribution in LY341495-induced neuronal activation.

## Materials and methods

### Animals

All experiments were performed using male, age-matched mGlu2- and mGlu3-KO and their corresponding WT (WT2 and WT3). mGlu2 mice were obtained from the University of Kyoto, Japan (Yokoi et al. 1996). Mice were backcrossed up to the 17th generation on C57BL/6J genetic background and bred in a specific pathogen-free (SPF) breeding colony. mGlu3 knockout mice were generated by targeted disruption of exon II of the Grm3 gene as recently described (Corti et al. 2007). All procedures used in this study were approved by the national Ethical Committee on Animal Care and Use (Bundesministerium für Wissenschaft und Verkehr, Kommission für Tierversuchsangelegenheiten, Austria) and are in compliance with the "Principles of laboratory animal care".

### c-Fos immunohistochemistry

All experiments were done between 8:00 and 12:00 A.M. Mice were injected (10 µl/g) with vehicle (veh) or LY341495 (3 mg/kg, i.p.), respectively, and subsequently returned to their home cage. Two hours after drug administration, mice were deeply anaesthetized with an overdose of sodium pentobarbital and transcardially perfused with 20 ml of 0.9% saline followed by 20 ml of 4% paraformaldehyde. Brains were then removed and postfixed at 4°C overnight in the fixative. Coronal sections (100 µm) were cut using a vibratome (Ted Pella, Redding, CA, USA) and collected in 0.1 M sodium phosphate buffer. The sections were processed for c-Fos immunoreactivity as described previously (Singewald et al. 2003). Briefly, sections were incubated for 48 h in a polyclonal primary antibody (sc-52, Santa Cruz Biotechnology, Santa Cruz, CA, USA) diluted 1:20,000 in buffer A (pH 7.4) containing 0.1 M NaCl, 5 mM KCl, 8 mM $Na_2HPO_4$, 15 mM $NaH_2PO_4$, 10 mM Tris–HCl, 0.3% Triton X-100, and 0.04% thimerosal. The rabbit primary antibody was raised

against a peptide in the amino terminus of human c-Fos p62 identical to the corresponding mouse sequence and does not cross-react with c-Fos B, Fra-1, or Fra-2. The sections were then rinsed and incubated with a biotinylated goat anti-rabbit secondary antibody (Vector Laboratories, Burlingame, CA, USA) for 24 h. An avidin–biotin–horseradish peroxidase procedure with 3,3′-diaminobenzidine as the chromogen was used to visualize the immunoreactivity.

### mGlu2/3 immunohistochemistry

Five adult male mice for each strain, (three for light microscopy and two for electron microscopy) were deeply anesthetized with thiopenthal (thiopentone sodium; 100 mg/kg, i.p) and transcardially perfused with 0.1 M phosphate-buffered 0.9% saline, followed for 10 min by a fixative composed of 4% paraformaldehyde, ~0.2% picric acid made up in 0.1 M phosphate buffer (PB, pH 7.2); only for those used for electron microscopy (EM), 0.05% glutaraldehyde was added to the fixative. Brains were quickly removed, extensively rinsed in PB and sectioned in the coronal plane at 40 or 70 μm thickness on a vibratome (Leica, Vienna, Austria). Immunocytochemical procedures were as described earlier (Corti 2002). Briefly, sections were pre-incubated (1 h) with 2% normal goat serum (NGS) in 0.1 M Tris-buffered saline (TBS) and subsequently incubated (72 h, 4 C) with a polyclonal antibody anti-mGlu2/3 (Chemicon, Temecula, CA, USA) diluted 1:500 in 1% NGS-50 mM TBS. Triton-X 100 (0.1%) was added when the sections were prepared only for light microscopy. Immunohistochemical reactions were carried out using either the avidin–biotin–HRP complex method (ABC, Elite kit, Vector) or Cy3™-conjugated secondary antibodies (diluted 1:400; Jackson ImmunoResearch, West Grove, PA, USA). Pre-embedding immunocytochemical reactions were performed using the avidin–biotin–HRP complex method. Sections were then subjected to 2% $OsO_4$ in 0.1 M PB and then contrasted with uranyl acetate (1%), dehydrated and embedded in Durcupan ACM (Fluka). Ultrathin sections (70 nm) were collected on pioloform-coated copper slot grids and analyzed by using a Zeiss CM120 electron microscope.

### Data analysis

Cells containing a nuclear brown-black reaction product were considered positive for c-Fos-immunoreactivity and are referred to hereafter as c-Fos positive cells. The anatomical localization of c-Fos-positive cells was aided by using the illustrations in a stereotaxic atlas (Franklin and Paxinos 1997). The staining procedure generally yielded low background staining. Moreover, we observed differential staining intensities of c-Fos positive cells as shown in the high magnification images of Fig. 1 (b and d). All cells clearly distinguishable from background staining were bilaterally counted in each region of interest within a defined area (0.01 $mm^2$) from one to two sections per mouse depending on the brain area under investigation.

### Drug dilutions

LY341495 (Tocris, Ellisville, MO, USA) was freshly dissolved in saline, and the pH value was adjusted with 0.1 M NaOH to 7.0. Veh was prepared accordingly except that LY341495 was omitted.

### Statistical analysis

Results are presented as means±SEM. Data analysis using the Kolmogorov–Smirnov test revealed nonparametric distribution in several brain regions. Therefore, overall statistical analysis was performed using the Kruskal–Wallis test for nonparametric data followed by Mann–Whitney *U* test to detect statistically significant differences within the groups. *P* values less than 0.05 were considered statistically significant.

## Results

### LY341495-induced c-Fos expression in WT mice

c-Fos expression in WT mice following veh application was generally rather low and indistinguishable between the two WT or KO strains or between the KO strains and corresponding WT strains. Therefore, the data of veh-treated animals were pooled (WT2/3, KO2/3) and served as veh control groups for the treatment with LY341495 (Table 1). Significant effects of LY341495 treatment were revealed by Kruskal–Wallis test in WT mice in 68 out of 92 areas quantified. Subsequent Mann–Whitney *U* test showed that this was due to increased LY341495-induced c-Fos expression in WT2 and WT3 compared to WT2/3 veh. As expected, WT2 and WT3 did not show statistically significant differences in LY341495-induced c-Fos expression. Data for all 92 brain areas analyzed are presented in Table 1. Compared to veh-treated WT2/3, WT2 and WT3 displayed robust increases of c-Fos expression following LY341495 application in all forebrain cortical areas investigated, such as the infralimbic cortex (10.1 vs. 18.7 and 15.8), the cingulate cortex (11.4 vs. 26.8 and 23.2), and the caudal primary motor cortex (1.4 vs. 24.2 and 20.2). In addition, LY341495 induced c-Fos expression in all investigated subregions of the nucleus accumbens and striatum. WT2 and WT3 mice treated with LY341495 also displayed increased c-Fos expression in various subcortical forebrain areas such as the ventral lateral septal nucleus (14.1 vs. 20.3 and 21.3) and

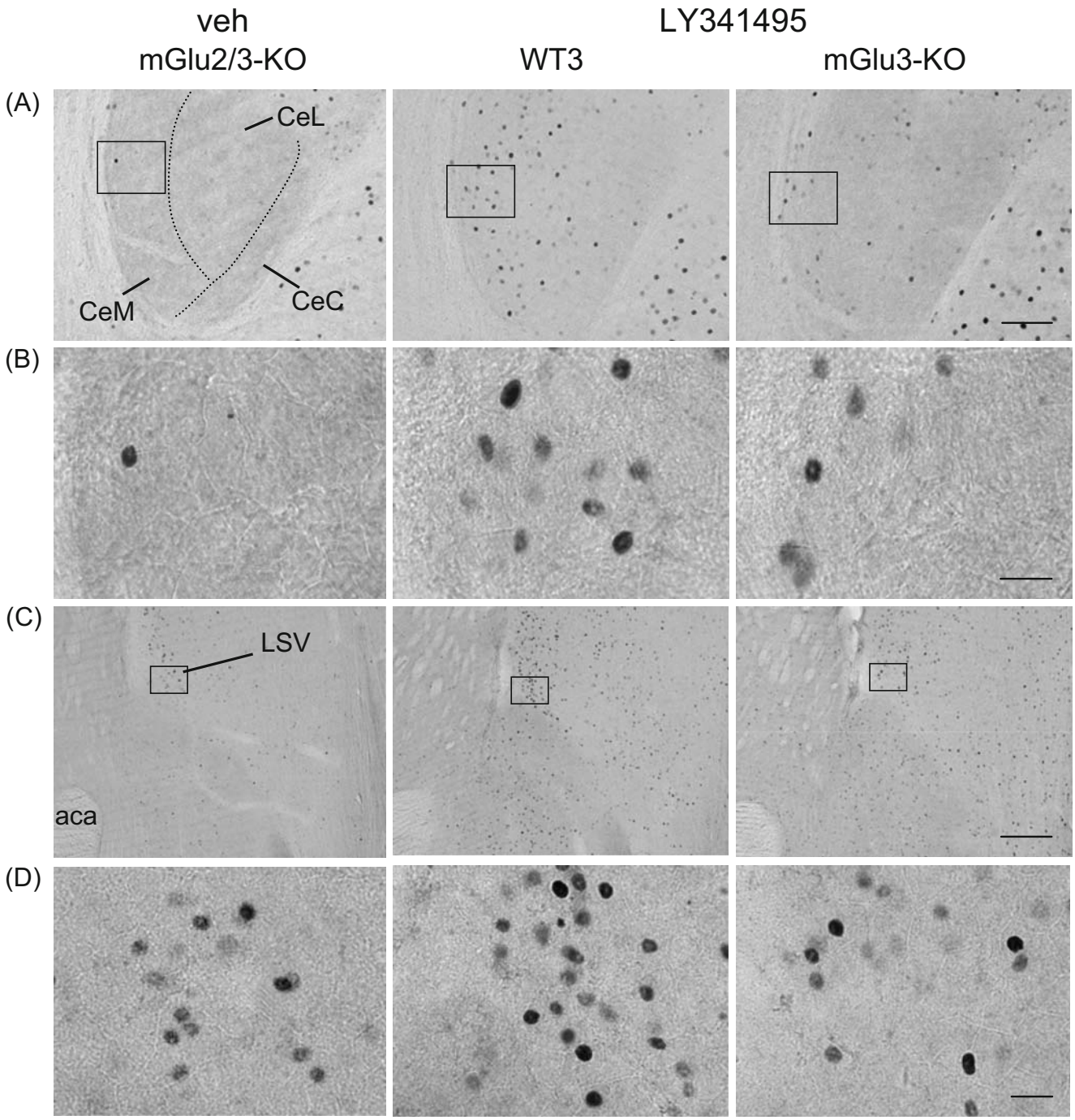


**Fig. 1** Effect of LY341495 on c-Fos expression in wild-type (*WT3*, *middle column*) and mice lacking mGlu3 (*mGlu3-KO*, *right column*). The effect of vehicle (*veh*) in the KO groups is shown as a representative example in the left column. Brain areas displayed are the medial central amygdala (CeM, **a**, **b**) and the ventral lateral septal nucleus (LSV, **c**, **d**). mGlu3-KO mice treated with LY341495 show decreased Fos expression compared to WT in both brain areas. **b** and **d** show high magnification images of *boxed areas* of (**a** and **c**). *CeL* Lateral central amygdala, *CeC* capsular central amygdala, *aca* anterior commissure, *anterior*, *scale bars*: 100 μm (**a**), 20 μm (**b**,**d**), 200 μm (**c**)

the lateral bed nucleus of the stria terminalis (6.9 vs. 12.7 and 11.8). All investigated hippocampal areas, apart from the ventral dentate gyrus, showed significant c-Fos induction following LY341495 treatment, e.g., the CA1 region of the pyramidal cell layer (2.8 vs. 19.3 and 17.8). Among the investigated subareas of the amygdala were the lateral, the medial, the basolateral, and the central nucleus, in which c-Fos expression was also quantified at different rostro-caudal levels. LY341495-induced c-Fos expression was noted at all levels in medial and basolateral nuclei, whereas in the lateral nucleus, this was observed at rostral areas only. Since c-Fos expression in the central amygdala (CeA) was

**Table 1** Overview of c-Fos expression in wild-type (WT2/3) and mice lacking mGlu2 or mGlu3 (mGlu-KO2/3) in the investigated brain areas following application of vehicle (veh) and LY341495

| Brain area | WT2/WT3 veh | WT2 LY341495 | WT3 LY341495 | mGlu2/3-KO veh | mGlu2-KO LY341495 | mGlu3-KO LY341495 |
|---|---|---|---|---|---|---|
| Forebrain | | | | | | |
| Cortical areas | | | | | | |
| Infralimbic cortex | 10.1±0.7 | 18.7±1.1** | 15.8±0.6** | 9.1±0.6 | 15.3±1.1** | 16.0±1.2** |
| Prelimbic cortex | 10.6±0.6 | 17.0±1.0** | 14.8±1.3* | 11.0±0.5 | 16.0±0.9** | 16.0±0.8** |
| Claustrum | 4.1±0.8 | 15.0±0.8** | 14.8±1.1** | 5.6±0.4 | 14.5±1.1** | 13.3±1.2** |
| Primary motor cortex, rostral | 0.9±0.3 | 16.7±2.5** | 16.8±2.7** | 0.9±0.3 | 17.0±3.8** | 17.1±2.5** |
| Primary motor cortex, caudal | 1.4±0.7 | 24.2±1.5** | 20.2±2.0** | 2.9±1.0 | 19.9±2.0** | 22.0±1.5** |
| Secondary motor cortex, rostral | 2.8±0.8 | 14.0±2.6** | 13.6±1.4** | 2.5±0.7 | 13.6±2.0** | 11.8±0.9** |
| Cingulate cortex | 11.4±0.9 | 26.8±2.1** | 23.2±2.0** | 8.7±0.6 | 23.6±2.0** | 21.1±2.9** |
| Piriform cortex, rostral | 13.4±0.9 | 36.7±1.6** | 35.3±2.3** | 13.7±1.5 | 36.1±3.1** | 33.3±5.8* |
| Piriform cortex, caudal | 8.4±0.5 | 30.5±1.9** | 28.2±3.9** | 9.3±0.9 | 31.6±4.4** | 26.0±1.6** |
| Somatosensory cortex 1, barrel field | 2.1±0.5 | 34.2±2.3** | 32.0±3.0** | 1.3±0.6 | 25.9±3.3** | 34.6±1.6** |
| Nucleus accumbens, shell, rostral | 9.5±1.1 | 14.2±0.9* | 13.2±0.7* | 8.0±0.6 | 13.8±0.9** | 14.3±0.8** |
| Nucleus accumbens, core, rostral | 0.4±0.3 | 6.2±0.7** | 5.7±0.6** | 0.1±0.1 | 6.1±0.5** | 5.7±0.7** |
| Nucleus accumbens, shell, caudal | 9.6±0.7 | 15.7±0.9** | 15.7±1.0** | 8.1±0.7 | 15.3±1.4** | 13.8±1.0** |
| Nucleus accumbens, core, caudal | 0.6±0.6 | 9.5±0.4** | 8.5±1.0** | 0.7±0.5 | 8.1±0.6** | 9.6±0.5** |
| Caudate putamen | | | | | | |
| Dorsolateral, rostral | 0.3±0.3 | 5.3±0.6** | 3.8±0.7** | 0.3±0.3 | 3.6±0.8** | 4.7±1.0** |
| Ventrolateral, rostral | 0.4±0.4 | 4.0±0.4** | 4.7±0.7** | 0.8±0.5 | 4.1±0.7** | 4.7±0.6** |
| Dorsomedial, rostral | 2.3±0.7 | 10.2±0.9** | 10.2±0.5** | 1.7±0.8 | 10.1±1.1** | 8.5±1.4** |
| ventromedial, rostral | 0.0±0.0 | 4.2±0.7** | 3.8±0.5** | 0.7±0.7 | 4.3±0.5** | 3.7±1.0* |
| Dorsolateral, caudal | 0.0±0.0 | 5.5±0.8** | 3.3±1.4* | 0.0±0.0 | 4.3±1.0** | 5.1±0.4** |
| Ventrolateral, caudal | 0.0±0.0 | 6.5±0.7** | 5.2±1.2** | 0.0±0.0 | 4.6±1.6** | 4.4±0.5** |
| Dorsomedial, caudal | 1.8±0.7 | 14.7±1.1** | 12.5±0.8** | 1.6±0.8 | 12.9±1.2** | 13.3±1.6** |
| Ventromedial, caudal | 0.3±0.3 | 9.7±0.9** | 9.2±1.1** | 0.0±0.0 | 8.0±1.2** | 9.1±1.0** |
| Lateral septal nucleus, dorsal | 4.6±0.3 | 9.0±0.4** | 9.0±0.9** | 4.5±0.6 | 8.5±0.6** | 8.2±0.7** |
| Lateral septal nucleus, ventral | 14.1±1.0 | 20.3±1.4** | 21.3±0.8** | 12.7±0.6 | 19.6±0.8** | 14.9±1.4$^{\#\#}$ |
| Lateral septal nucleus, intermediate | 6.1±0.5 | 12.3±1.2** | 12.0±1.6** | 6.1±0.7 | 12.5±1.1** | 10.7±0.7** |
| Bed nucleus stria terminalis, medial, ventral | 3.8±0.7 | 6.3±0.8* | 6.5±0.4* | 5.0±0.5 | 5.9±0.5 | 7.3±0.4* |
| Bed nucleus stria terminalis, lateral, posterior | 6.9±0.5 | 12.7±1.4** | 11.8±1.2* | 6.8±0.5 | 11.0±0.7** | 12.7±1.0** |
| Medial septal nucleus | 1.5±0.5 | 6.5±0.4** | 6.2±0.5** | 1.5±0.7 | 5.6±0.7** | 7.0±0.7** |
| Lateral preoptic area | 3.6±0.7 | 11.0±1.8** | 10.3±1.1** | 2.3±0.8 | 8.4±0.7** | 7.9±0.7** |
| Medial preoptic area | 5.4±0.6 | 10.5±2.1* | 7.0±1.1 | 3.4±0.9 | 10.0±2.0* | 10.1±1.5** |
| Hippocampal formation | | | | | | |
| Pyramidal cell layer, CA1 region | 2.8±0.5 | 19.3±0.8** | 17.8±1.8** | 2.8±0.5 | 12.9±2.5** | 17.4±1.5** |
| Pyramidal cell layer, CA3 region | 0.0±0.0 | 2.0±0.7** | 2.3±0.2*** | 0.0±0.0 | 1.3±0.5* | 2.4±0.5** |
| Granular layer, dentate gyrus, dorsal | 7.3±0.4 | 11.5±1.1** | 11.3±0.4** | 7.8±0.5 | 11.3±0.6** | 11.7±0.6** |
| Pyramidal cell layer, ventral | 4.9±0.5 | 14.0±1.1** | 12.3±1.5** | 3.4±0.7 | 11.5±1.1** | 9.7±1.8** |
| Granular layer, dentate gyrus, ventral | 1.5±0.6 | 1.7±0.6 | 2.5±0.7 | 1.4±0.5 | 2.5±0.8 | 1.4±0.5 |
| Amygdala | | | | | | |
| Lateral nucleus, rostral | 3.1±0.5 | 9.5±1.2** | 8.5±0.7** | 4.0±0.6 | 7.1±0.7** | 9.5±1.2** |
| Medial nucleus, rostral | 5.3±0.4 | 12.7±0.8** | 13.2±2.0** | 5.0±0.5 | 12.6±1.3** | 15.7±2.1** |
| Basolateral nucleus, rostral | 3.5±0.5 | 11.2±1.5** | 11.8±0.8** | 3.4±0.5 | 10.9±1.7** | 10.4±1.2** |
| Central nucleus, capsular, rostral | 4.4±0.8 | 5.5±0.8 | 5.2±1.0 | 2.9±0.7 | 6.8±1.3 | 4.7±0.8 |
| Central nucleus, lateral, rostral | 1.5±0.4 | 9.3±0.8** | 8.5±0.8** | 1.6±0.3 | 9.1±0.8** | 6.8±0.9** |
| Central nucleus, medial, whole area, rostral | 5.0±2.2 | 40.2±1.7** | 36.5±2.5** | 4.0±1.0 | 37.5±1.3** | 13.7±2.5**$^{,\#\#}$ |
| Lateral nucleus, caudal | 5.3±0.4 | 6.5±0.9 | 6.3±0.6 | 5.5±0.3 | 5.3±0.5 | 7.1±0.8 |
| Medial nucleus, caudal | 5.3±0.4 | 11.2±1.2** | 9.4±0.8** | 5.0±0.5 | 8.8±0.6** | 11.7±1.1** |
| Basolateral nucleus, caudal | 3.5±0.5 | 11.5±1.0** | 11.3±0.9** | 3.4±0.5 | 11.5±0.8** | 11.3±1.1** |
| Central nucleus, capsular, caudal | 4.4±0.6 | 4.5±0.6 | 4.0±0.4 | 3.8±0.9 | 3.6±0.5 | 3.3±0.6 |
| Central nucleus, lateral, caudal | 2.9±0.4 | 8.5±0.7** | 8.2±1.1** | 2.1±0.4 | 7.0±0.3** | 7.2±1.4* |
| Central nucleus, medial, whole area, caudal | 5.5±1.0 | 35.7±1.3** | 38.7±0.9** | 5.3±1.0 | 34.9±1.5** | 14.7±2.6**$^{,\#\#}$ |

**Table 1** (continued)

| Brain area | WT2/WT3 veh | WT2 LY341495 | WT3 LY341495 | mGlu2/3-KO veh | mGlu2-KO LY341495 | mGlu3-KO LY341495 |
|---|---|---|---|---|---|---|
| Diencephalon | | | | | | |
| Thalamus | | | | | | |
| Paraventricular nucleus, anterior, rostral | 23.9±2.3 | 20.5±2.1 | 22.2±1.0 | 23.1±1.2 | 19.9±2.0 | 18.6±3.0 |
| Paraventricular nucleus, anterior, caudal | 14.8±1.7 | 20.0±1.5 | 20.0±1.5 | 11.3±1.8 | 17.8±1.0** | 18.0±1.4* |
| Paracentral nucleus | 4.3±1.3 | 13.5±2.0** | 15.3±2.6** | 6.1±1.7 | 13.0±1.7* | 13.6±2.4* |
| Central medial nucleus, rostral | 12.4±1.2 | 19.8±1.9** | 17.3±1.2** | 11.0±0.6 | 19.1±1.9** | 19.9±2.8** |
| Central medial nucleus, caudal | 5.3±0.7 | 15.8±1.5** | 13.5±0.8** | 5.8±1.1 | 14.8±1.3** | 15.0±1.1** |
| Lateral habenular nucleus | 3.4±0.6 | 4.8±1.3 | 3.8±1.0 | 3.4±0.5 | 8.0±3.0 | 4.9±1.4 |
| Ventromedial nucleus | 0.0±0.0 | 9.7±1.0** | 12.2±1.5** | 0.6±0.6 | 9.1±2.1** | 18.0±7.7** |
| Zona incerta | 5.9±0.6 | 15.0±2.0** | 11.2±1.0** | 5.5±0.8 | 14.4±1.8** | 10.7±1.1** |
| Mediodorsal nucleus | 9.4±1.8 | 10.5±1.1 | 14.7±3.3 | 8.0±1.5 | 8.9±1.4 | 12.7±2.0 |
| Reticular nucleus | 1.1±0.8 | 5.2±0.7** | 3.2±0.6* | 1.8±0.9 | 3.3±0.7 | 4.0±1.2 |
| Hypothalamus | | | | | | |
| Suprachiasmatic nucleus | 47.1±9.6 | 38.3±2.4 | 37.8±3.1 | 36.3±5.4 | 40.9±5.0 | 38.7±3.0 |
| Paraventricular nucleus, parvocellular | 3.7±0.4 | 5.3±0.5 | 4.7±1.2 | 3.3±0.6 | 4.0±0.5 | 5.1±0.6 |
| Paraventricular nucleus, magnocellular | 15.1±1.2 | 16.2±1.5 | 15.5±2.2 | 16.5±1.3 | 17.5±1.5 | 15.3±0.9 |
| Anterior area, central | 7.1±0.3 | 9.2±0.3 | 8.0±0.9 | 5.9±1.1 | 9.3±0.5 | 8.9±1.5 |
| Lateral area, rostral | 5.9±0.8 | 8.7±1.0 | 8.0±0.7 | 5.5±0.9 | 9.9±0.9** | 7.0±1.1 |
| Lateral area, caudal | 7.1±0.7 | 11.8±0.9** | 13.3±1.0** | 7.0±0.8 | 12.4±0.7** | 12.6±0.9** |
| Dorsomedial nucleus | 11.9±1.0 | 13.2±0.8 | 12.8±1.7 | 12.9±1.2 | 11.9±0.9 | 14.1±1.5 |
| Ventromedial nucleus | 8.0±0.7 | 6.0±0.9 | 5.5±0.9 | 7.8±0.8 | 5.5±0.8 | 3.6±0.5 |
| Midbrain, brainstem, pons | | | | | | |
| Ventral tegmental area | 0.0±0.0 | 0.3±0.2 | 2.7±1.0* | 0.3±0.3 | 1.0±0.5 | 3.6±0.9** |
| Substantia nigra, pars compacta | 0.0±0.0 | 1.0±0.4* | 0.5±0.5 | 0.0±0.0 | 0.6±0.4 | 0.3±0.3 |
| Substantia nigra, pars reticulata | 0.0±0.0 | 0.0±0.0 | 0.8±0.5 | 0.0±0.0 | 0.0±0.0 | 0.1±0.1 |
| Interpeduncular nucleus | 4.9±0.8 | 26.7±4.8** | 19.3±2.2** | 7.0±1.4 | 17.1±2.2** | 17.4±3.3* |
| Superficial gray, superior colliculus | 9.9±0.9 | 12.2±0.9 | 10.2±0.6 | 10.8±0.5 | 12.0±1.1 | 15.9±1.1** |
| Deep gray layer, superior colliculus | 2.6±0.5 | 9.0±0.7** | 8.6±0.4** | 1.8±0.7 | 8.0±0.9** | 8.9±0.5** |
| Edinger–Westphal nucleus | 14.6±1.4 | 8.8±1.4 | 10.3±1.8 | 8.0±2.1 | 10.9±1.6 | 6.9±0.6 |
| Pentane nuclei, rostral | 18.9±2.6 | 23.8±3.0 | 18.7±2.7 | 16.8±1.8 | 27.1±2.9 | 25.4±2.8 |
| Pentane nuclei, caudal | 16.8±2.4 | 23.0±10.0 | 32.8±6.0 | 13.0±2.8 | 30.0±5.2 | 30.7±5.5 |
| Raphe nuclei | | | | | | |
| Caudal linear nucleus | 2.4±1.0 | 12.2±3.3** | 7.7±1.5* | 2.6±0.8 | 8.1±0.8** | 9.3±1.1** |
| Paramedian nucleus | 3.0±0.3 | 11.5±2.0** | 9.8±1.8** | 3.5±0.5 | 9.5±1.3** | 5.1±0.7 |
| Median nucleus | 4.5±0.6 | 15.0±2.4** | 12.5±1.1** | 4.0±1.3 | 10.6±1.5** | 15.7±1.8** |
| Dorsal nucleus, rostral | 5.4±0.8 | 15.7±1.3** | 14.3±1.0** | 6.4±0.4 | 12.8±1.2** | 15.6±2.2** |
| Dorsal nucleus, ventrolateral, caudal | 2.1±1.0 | 10.7±1.3** | 8.0±1.5** | 0.9±0.6 | 6.6±1.5** | 9.9±1.1** |
| Dorsal nucleus, dorsal, caudal | 1.6±0.6 | 6.8±1.1** | 4.0±0.5* | 1.6±0.6 | 5.9±1.2* | 6.6±1.4** |
| Dorsal nucleus, inferior | 8.4±0.9 | 20.0±1.9** | 15.0±1.0** | 8.5±1.1 | 18.6±2.4** | 18.3±1.4** |
| Lateral periaqueductal gray | 11.0±0.9 | 12.8±0.7 | 11.5±1.0 | 10.1±0.7 | 12.4±0.7* | 11.3±0.7 |
| Ventrolateral periaqueductal gray | 9.9±0.4 | 14.0±1.0** | 15.3±1.9* | 8.1±1.2 | 12.8±1.0* | 12.4±0.9* |
| Dorsomedial periaqueductal gray | 7.6±1.7 | 15.0±0.6* | 12.2±1.6* | 6.6±0.8 | 12.3±1.7* | 13.0±1.4** |
| Dorsolateral periaqueductal gray | 5.4±0.7 | 6.7±0.4 | 6.3±1.0 | 5.0±0.5 | 7.1±0.5* | 6.1±0.7 |
| Lateral parabrachial nucleus, dorsal | 10.0±2.6 | 16.8±1.5* | 13.0±1.3* | 10.1±0.8 | 12.8±1.5 | 11.4±2.0 |
| Lateral parabrachial nucleus, external | 7.5±2.0 | 22.5±1.6** | 20.8±1.8** | 3.5±1.0 | 12.1±1.2**# | 9.4±1.2**# |
| Central nucleus, inferior colliculus | 9.4±1.6 | 5.8±0.7 | 7.5±1.2 | 8.8±0.6 | 8.3±0.8 | 9.1±1.6 |
| Locus coeruleus | 5.3±1.9 | 10.7±1.5 | 7.7±0.4 | 2.4±0.8 | 7.3±1.7 | 6.6±0.6 |
| Nucleus of the solitary tract | 5.7±1.1 | 13.5±3.0* | 8.0±1.3 | 3.1±0.8 | 7.0±2.1 | 14.5±3.9 |

(WT: $n$=8; ko2/3: $n$=8) or LY341495 (3 mg/kg) (WT2: $n$=6, WT3: $n$=6; mGlu2-KO: $n$=8, mGlu3-KO: $n$=7). The number of c-Fos-positive cells/0.01mm$^2$ is given as mean±SEM. Statistical analysis was performed using Kruskal–Wallis test followed by Mann–Whitney $U$ Test

*$p$<0.05

**$p$<0.01 LY341495 vs. veh

$^{\#}p$<0.05

$^{\#\#}p$<0.01 KO vs. WT

not evenly distributed, we have further subdivided the CeA according to the atlas of Franklin and Paxinos (1997). Indeed, we found LY341495-induced increases in c-Fos expression particularly in the medial part (CeM) and, to a lesser extent, in the lateral part (CeL), but not in the capsular part (CeC) of the CeA. Counting the whole area of the CeM revealed dramatic increases in LY341495-induced c-Fos expression compared to veh treatment (5.5 vs. 35.7 and 38.7). Moreover, we found increases following LY341495 treatment in thalamic areas such as the paracentral nucleus and the central medial nucleus. Hypothalamic areas generally showed low c-Fos responses upon administration of LY341495. For example, the group II mGlu antagonist failed to trigger neuronal activation in the paraventricular hypothalamic nuclei. Slightly enhanced c-Fos expression was observed in the caudal but not rostral parts of the lateral hypothalamus. Finally, LY341495 induced c-Fos expression in midbrain areas such as raphe nuclei and the lateral parabrachial nucleus (Table 1).

In contrast, in 24 out of 92 investigated areas, LY341495 failed to induce c-Fos expression in WT mice (Table 1). Brain areas displaying no LY341495-induced c-Fos induction included the ventral granular layer of the dentate gyrus, the capsular part of the CeA, the lateral amygdala, the paraventricular hypothalamic nucleus, and the locus coeruleus. Furthermore, we did not observe differences in c-Fos expression between veh and LY341495 treatment in thalamic areas such as the lateral habenular nucleus and the mediodorsal nucleus, hypothalamic areas including the anterior and the lateral area and the dorsomedial nucleus as well as midbrain areas such as the substantia nigra (Table 1).

## Contribution of mGlu2 and mGlu3 to LY341495-induced c-Fos expression

Similar to WT mice, treatment with veh caused generally low c-Fos induction in the majority of investigated brain areas and was indistinguishable in both KO strains. Accordingly, the veh data were pooled (KO2/3; Table 1). Moreover, c-Fos expression did not differ in WT and KO mice following veh treatment (Table 1). LY341495-induced c-Fos response was markedly attenuated (down to veh levels) in the CeM, and the ventral lateral septal nucleus (LSV) in mGlu3-KO mice compared to both WT strains and mGlu2-KO (Figs. 1, 3, Table 1). This effect was observed in the CeM of mGlu3-KO mice both at rostral and caudal levels (Table 1). In addition, in the lateral parabrachial nucleus (LPB), LY341495-induced c-Fos expression was significantly reduced in both KO strains compared to their corresponding WT (Figs. 2, 3, Table 1). Surprisingly, LY341495 enhanced c-Fos expression to a similar extent in both WT and KO strains in most of the areas investigated (Table 1).

In order to investigate further the mechanisms involved in LY341495-induced neuronal activation, we have analyzed the cellular and subcellular distribution of mGlu2 and mGlu3

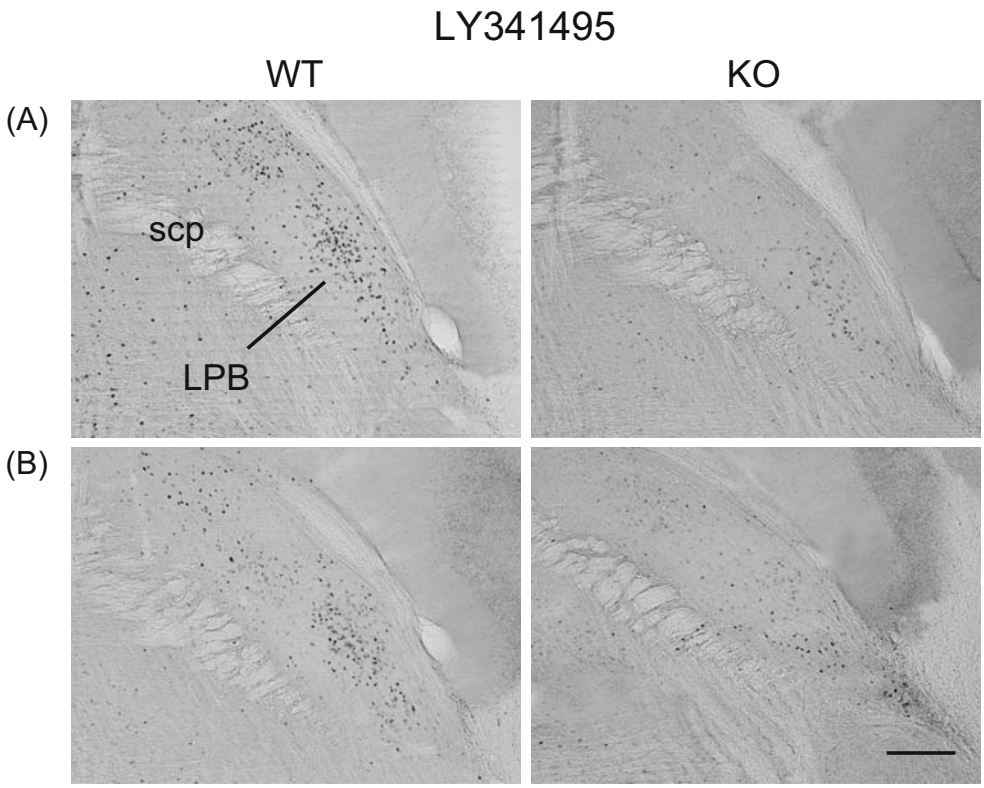


**Fig. 2** c-Fos expression following treatment with LY341495 (3 mg/kg) in wild-type (*WT*, *left column*) compared to mice lacking mGlus (*KO*, *right column*) in the lateral parabrachial nucleus (*LPB*). LY341495-induced Fos expression is decreased in mGlu2-KO compared to WT2 (**a**) and in mGlu3-KO compared to WT3 (**b**). *scp* Superior cerebellar peduncle, *scale bar*=200 μm

receptors in the amygdala of mGlu2- and mGlu3-KO mice by using an antibody for the C-terminal domain of the rat mGlu2 receptor, but which cross-reacts with mGlu3. This antibody has been well characterized previously (Ferraguti et al. 2001). The antibody produced intense labeling in the basolateral complex and moderate staining of the central nucleus of WT mice (Fig. 4a). No differences could be detected between WT2 and WT3. In contrast, in the mGlu3-KO, the immunolabeling corresponding to mGlu2 showed a preferential distribution in certain nuclear subdivision including the medial magnocellular component of the BLA and the CeL. The labeling was characterized by a punctate pattern in the neuropil (Fig. 4b). In the medial division of the CeA, the immunostaining was significantly weaker compared to the CeL. In mGlu2-KO, the immunolabeling for mGlu3 was found more homogeneously distributed. Likewise for mGlu2, immunoreactivity (IR) for mGlu3 was mostly observed in the neuropil with a punctate staining pattern (Fig. 4c).

The subcellular localization of mGlu3 immunoreactivity in the CeM of mGlu2-KO mice was examined by pre-embedding immunoelectron microscopy. Peroxidase reaction end product for mGlu3 was observed most frequently in small profiles of glial processes (Fig. 5a). In neuronal profiles, mGlu3-IR was detected only in postsynaptic elements such as small dendritic shafts and spines (Fig. 5b–c). Conversely, the subcellular localization of mGlu2-IR in the CeM of mGlu3-KO mice was limited to infrequent presynaptic elements, which consisted of small unmyelinated axons and presynaptic boutons. Immunolabeled axon terminals formed mostly asymmetric synapses with spines or small dendrites, and although infrequently, also symmetric synapses on dendrites, (Fig. 6).

## Discussion

Here, we report that blockade of group II mGlus by LY341495 caused increased c-Fos expression in a large number (68 out of 92) of brain areas, many of which are particularly associated with anxiety-related behavior. In addition, our experiments involving mice lacking mGlu2 or mGlu3 revealed that the LY341495-induced c-Fos expression was predominantly mediated via mGlu3 in the CeM and the LSV and via both subtypes in the LPB. Moreover, immunohistochemical studies at both light and electron microscopy revealed a prevailing presence of mGlu3 receptors in the CeM on both glial processes and postsynaptic neuronal elements. Conversely, in this area, mGlu2-IR was weak and associated only to presynaptic elements.

### LY341495-induced c-Fos expression in WT mice

Activation of presynaptic mGlu2/3 has been shown to provide a negative feedback mechanism controlling the release of neurotransmitters such as glutamate, GABA, or dopamine (Anwyl 1999; Cartmell and Schoepp 2000). On the other hand, stimulation of postsynaptic mGlu2/3 was found to

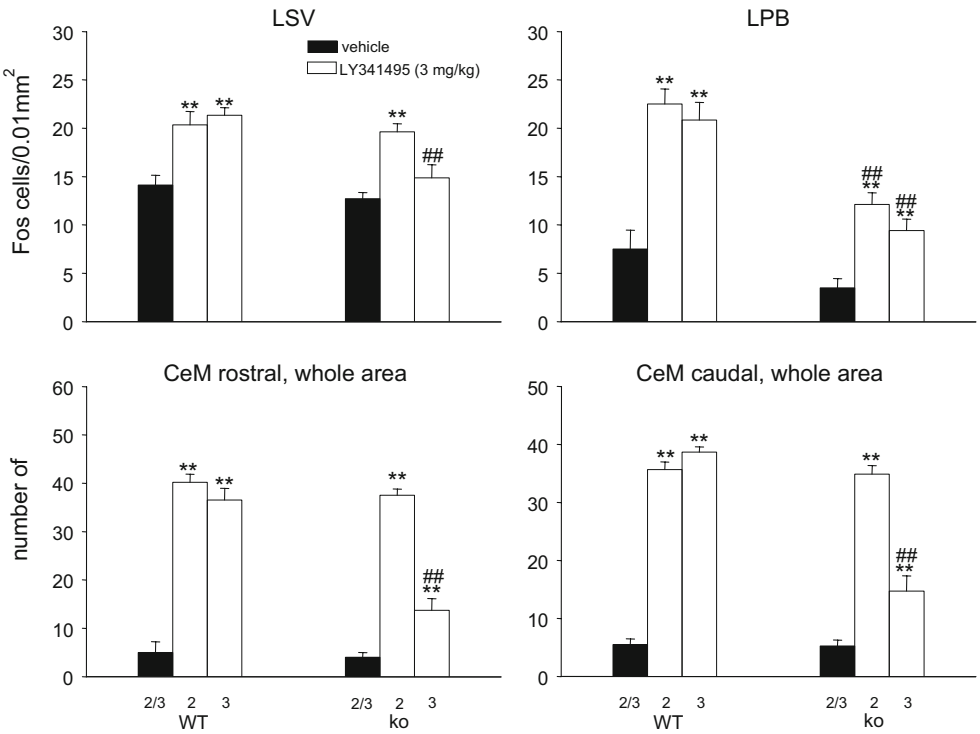


**Fig. 3** Quantification of LY341495-induced Fos expression in mGlu2- and mGlu3-KO mice compared to WT controls. *Black bars* indicate treatment with vehicle, *white bars* indicate LY341495 treatment (3 mg/kg). Note that in the ventral lateral septal nucleus (*LSV*) and the lateral parabrachial nucleus (*LPB*), the Fos cells/0.01 mm$^2$ are indicated, while in the rostral and caudal medial central amygdala (*CeM*), the whole area was quantified. Data are presented as mean±SEM. **$p<$ 0.01 LY341495 vs. veh, ##$p<$ 0.01 KO vs. WT, Kruskal–Wallis test followed by Mann–Whitney *U* test

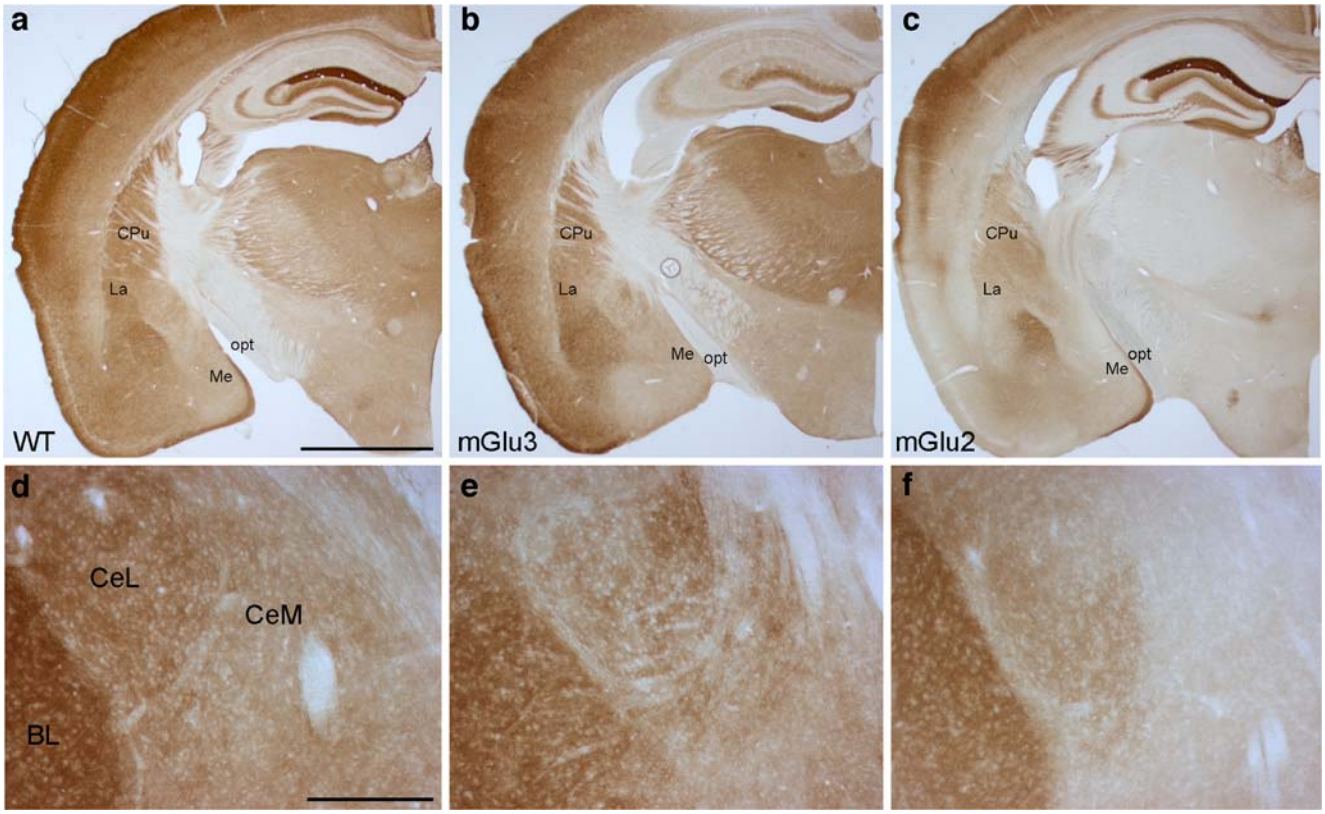


**Fig. 4** Immunohistochemical localization of mGlu2 and mGlu3 receptors in the CeA of wild-type, mGlu2-and mGlu3-KO mice. **a**–**c** Low magnification microphotographs of mouse hemisections of wild-type (**a** only WT2 is depicted here), mGlu2-KO (**b**), and mGlu3-KO (**c**) immunolabeled for mGlu2/3. Note the distinctive labeling corresponding to mGlu3 (**b**) and mGlu2 (**c**) in the hippocampal formation, thalamus, and amygdala. **d**–**e** Immunoreactivity for mGlu2 and mGlu3 is observed as punctate staining in the neuropil of the Ce and basolateral nucleus of the amygdala (*BL*). In wild-type mice (**d**) intense labeling can be observed in the BL and *CeL*, whereas the *CeM* shows only moderate staining. In mGlu2-KO (**e**), mGlu3 staining resemble that in the WT with moderate labeling in the *CeM*. Conversely, in mGlu3-KO (**f**) mGlu2 staining is intense in *CeL* but very weak in the *CeM*. *BL* Basolateral nucleus of the amygdala, *CeL* central nucleus of the amygdala, lateral subdivision, *CeM* central nucleus of the amygdala, medial subdivision, *CPu* caudate–putamen, *La* lateral nucleus of the amygdala, *Me* medial nucleus of the amygdala, *opt* optic tract. *Scale bars*: **a**–**c** 1 mm; **d**–**f** 250 μm

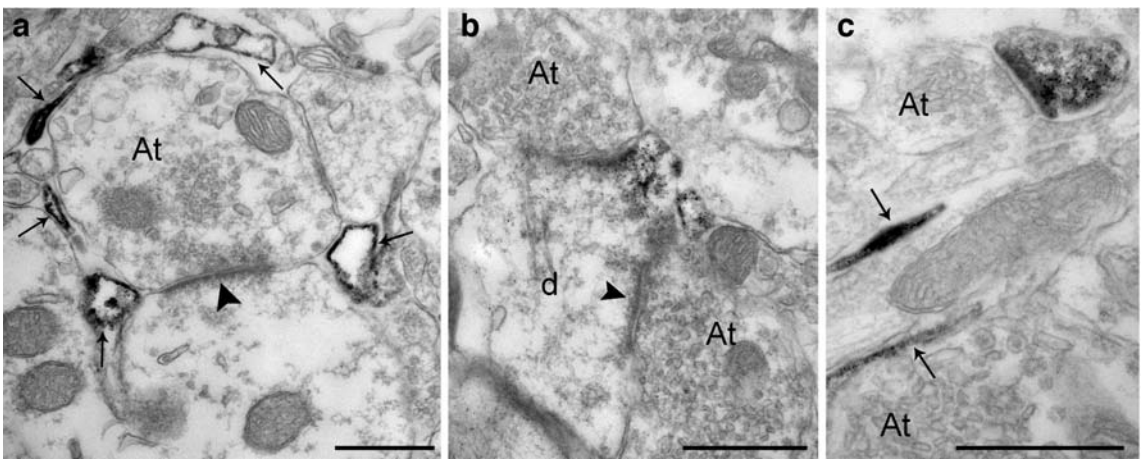


**Fig. 5** Ultrastructural localization of mGlu3-IR in the CeM of mGlu2-KO mice. **a** Immunoreactivity for mGlu3 is observed in small glial processes (indicated by *small arrows*) surrounding pre- and postsynaptic elements forming an asymmetric synapse (*arrowhead*). **b** Peroxidase end product indicating mGlu3-IR can be seen at extrasynaptic locations in dendritic shafts as well as **c** in spines. *At* Axon terminal. *Scale bars*: 500 nm

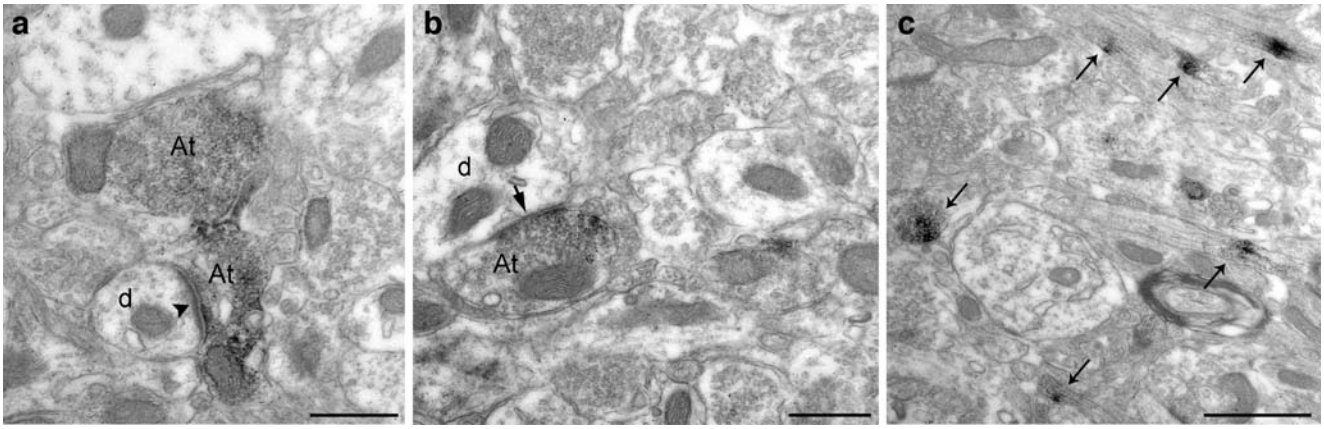


**Fig. 6** Ultrastructural localization of mGlu2-IR in the CeM of mGlu3-KO mice. **a** Immunoperoxidase labeling for mGlu2 can be observed in two axon terminals (*At*), one of which makes an asymmetrical synapse with a small dendrite. **b** A mGlu2 immunolabeled bouton forms a symmetrical synapse with a small dendritic shaft. **c** Peroxidase end product can be observed in small unmyelinated axons (*arrows*). *Scale bars*: **a**–**b** 500 nm; **c** 1 μm

modulate neuronal excitability and plasticity via intracellular mechanisms such as modulation of ion channels (e.g., potassium) and adenylyl cyclase (Anwyl 1999; Schaffhauser et al. 1997; Schoepp et al. 1998). Thus, blockade of group II mGlu receptors by LY341495 may increase neuronal activation via multiple mechanisms involving pre- and/or postsynaptic sites either in neurons or in glial cells.

Consistent with the known widespread distribution of group II mGlus as revealed by in situ hybridization techniques (Ohishi et al. 1993a, b; Tanabe et al. 1993), immunohistochemistry (Petralia et al. 1996; Tamaru et al. 2001), and radioligand binding studies using both agonists (Mutel et al. 1998; Schaffhauser et al. 1998) and antagonists (Wright et al. 2001), we have observed a widespread increase in c-Fos expression induced by LY341495 in the brain, including numerous forebrain cortical areas, such as the prefrontal and the cingulate cortex, the nucleus accumbens, striatum, lateral septum, and bed nucleus of the stria terminalis, the central medial thalamic nucleus, the lateral hypothalamic area, the pyramidal cell layer of the hippocampal CA1 region, several amygdala and hindbrain areas including various raphe nuclei. On the other hand, only 24 regions, out of 92 regions quantified, did not show significant activation following LY341495 treatment, which included hypothalamic areas such as the paraventricular and the ventromedial nucleus, the ventral granular layer of the dentate gyrus, and the superficial grey of the superior colliculus.

Since many of the LY341495-induced activated areas including the amygdala, septum, prefrontal cortex, and hippocampus are critically involved in anxiety-related processing (Charney et al. 1998), it may be hypothesized that LY341495 exerts anxiogenic-like efficacy. Indeed, it has recently been shown that LY341495 elicits anxiogenic-like responses on the elevated plus maze, which was associated with a widespread increase in neuronal activation (Linden et al. 2005a). The pattern of LY341495-induced c-Fos expression described here is similar to the study from Linden and colleagues (Linden et al. 2005b), which have demonstrated an elevated c-Fos response in the lateral, medial, and capsular part of the CeA following treatment with LY341495. In our study, we have observed a more specific activation pattern involving the lateral and medial subdivisions of the CeA, but not the capsular part. Although there are unfortunately only a limited number of studies that have divided the CeA into subregions, it seems that anxiolytic drugs activate neurons primarily in the lateral CeA (Beck and Fibiger 1995; Cohen et al. 2003; Linden et al. 2004), which are presumably GABAergic (Hitzemann and Hitzemann 1999). At odds with our study, Linden and colleagues found that LY341495 induced neuronal activation also in thalamic areas such as the paraventricular nucleus and the mediodorsal nucleus, hypothalamic nuclei such as the dorsomedial nucleus, midbrain and hindbrain areas such as the substantia nigra or the locus coeruleus. A possible explanation for these discrepancies may be the different genetic background of the mice used in the two studies: Linden used the CD1 mouse strain, whereas for our study, we used mice back-crossed into the C57Bl/6 background. These two mouse strains show important behavioral differences in stress- and anxiety-related tests, such as predator-induced freezing and risk assessment and exploration in the light dark box (e.g., Yang et al. 2004; Kinsey et al. 2007), which may produce also differential neuronal activation upon exposure to stress and/or drugs. Indeed, a recent experiment carried out in our lab showed strain-dependent differential neuronal activation in response to stress, e.g., by exposure to aversive stimuli (Hetzenauer and Singewald, unpublished).

## Contribution of mGlu2 and mGlu3 to LY341495-induced neuronal activation

Since LY341495 affects mGlu2 and mGlu3 with similar efficacy (Kingston et al. 1998; Ornstein et al. 1998), we applied LY341495 to mice lacking mGlu2 or mGlu3 in order to determine the contribution of each subtype to LY341495-induced neuronal activation. We can assume that LY341495 mediates neuronal activation via mGlu2 in mGlu3-KO mice and via mGlu3 in mGlu2-KO mice (for evidence of low affinity binding of LY341495 to mGlu8 receptors see discussion below). The strong attenuation of LY341495-induced neuronal activation observed in the CeM and the lack of response in the LSV of mGlu3-KO mice, compared to WT, indicates that LY341495-mediated c-Fos expression in these areas depends primarily on mGlu3 receptors, absent in these mice. In addition, in both KO strains, LY341495 displayed a reduced c-Fos induction in the LPB, indicating the contribution of both subtypes to LY341495-induced neuronal activation.

Previous in situ hybridization studies have reported a lack of expression of mGlu2 and mGlu3 in neuronal profiles of the CeA (Ohishi et al. 1993a, b), whereas both immunohistochemical (Petralia et al. 1996; Tamaru et al. 2001) and radioligand binding studies using [3H]LY341495 (Wright et al. 2001) revealed low to moderate expression of both subtypes. However, so far, no ultrastructural data are available concerning group II mGlus in the rodent amygdala and in particular in the CeA. Only recently, evidence for glial as well as presynaptic and postsynaptic localization in the rat basolateral complex and bed nucleus of the stria terminalis has been reported (Muly et al. 2007). Here we demonstrate a moderate immunolabeling for mGlu2/3 receptors in the mouse CeA, with a prevailing presence of mGlu3 receptors in the CeM on both glial processes and postsynaptic neuronal elements, such as dendritic shafts and spines. Our findings on the subcellular distribution of group II mGlu receptors suggest that LY341495-induced neuronal activation results either from the modulation of a neuronal–glial intercommunication involving astroglial mGlu3 receptors or the removal of an inhibitory role mediated by postsynaptic mGlu3 receptors.

The CeA and the LS have been strongly implicated in anxiety-related processing. Lesions of the CeA have consistently been reported to elicit anxiolytic-like effects in various tasks such as the defensive-burying test (Roozendaal et al. 1991), drinking conflict tests (Moller et al. 1997; Oakes and Coover 1997), and conditioned fear (Goosens and Maren 2001). Moreover, lesions of the CeA cause reduced fear-related behavior in monkeys upon exposure to fearful stimuli such as snakes or human intruders (Kalin et al. 2004). In contrast, repeated electrical stimulation (i.e., kindling) of the CeA causes increased anxiety-related behavior (Kalynchuk et al. 1997). Interestingly, although the classical parameters of the elevated plus maze (i.e., percent open arm entries and percent time on open arms) pointed to an anxiolytic phenotype of CeA kindling, the authors postulated that anxiety-related behavior increases with the number of stimulations presented. Animals receiving low numbers of kindling procedures (e.g., 20) ventured the open arm attempting to search escape from the apparatus while they showed extreme escape-directed behavior and finally even jumped off the maze after higher repetitions of kindling (Kalynchu et al. 1997). In addition, lesions of the lateral septal nucleus exert anxiolytic-like behavior on the elevated plus maze (Menard and Treit 1996). In summary, anxiety-related behavior appears to be associated with neuronal activation in the CeA and the LS. If antagonism at mGlu3 receptors mediates neuronal activation in these two areas, hence contributing to the anxiogenic action of LY341495, mGlu3-KO mice should display reduced anxiety-related behavior in response to this drug. This hypothesis remains to be further investigated.

Given the widespread distribution of mGlu2 and mGlu3 receptors, it is rather surprising that both mGlu2-and mGlu3-KO mice showed reductions of LY341495-induced c-Fos expression only in few restricted areas (CeM, LSV and LPB). The vast majority of brain areas investigated displayed similar c-Fos responses following LY341495 treatment in WT and both group II mGlu null mouse strains. Several explanations may account for the observation that deletion of one subtype is not sufficient to cause reductions of LY341495-induced neuronal activation: (1) it is tempting to speculate that adaptive changes, such as the upregulation of the other subtype has occurred, thus compensating the lack of the ablated receptor. This issue is currently under investigation; preliminary experiments point to only a moderate upregulation of LY341495 binding sites in mGlu3-KO compared to WT, for example, in the hippocampus (Corti and Corsi, personal communication). (2) LY341495-mediated activation of mGlu8 receptors. Although LY341495 was shown to bind to mGlu8 at about tenfold higher concentrations than to mGlu2 and mGlu3 (Kingston et al. 1998; Ornstein et al. 1998; Wright et al. 2000), it cannot be ruled out that activation of mGlu8 contributes to LY341495-induced c-Fos expression particularly in mice lacking one subtype of group II mGlus, since ablation of one subtype may reduce the potential binding sites for LY341495 and therefore increase the likelihood of activation of mGlus other than group II. Moreover, mGlu8 has been shown to be co-expressed with group II mGlus in several regions analyzed in the present study including the cerebral cortex and the BLA (Corti et al. 1998). (3) a cross talk between the two subtypes, possibly involving different neuronal and glial elements, is necessary to produce a widespread neural activation. Studies with mice lacking both mGlu2 and mGlu3 would help to clarify these mechanisms.

In summary, we report that the selective mGlu2/3 antagonist LY341495 enhances neuronal activation in a variety of brain areas throughout the brain, many of which are associated with the processing of anxiety-related behavior. This is consistent with findings showing anxiogenic-like effects of LY341495 in the elevated plus maze (Linden et al. 2005a). Antagonists at group II mGlus, however, were also shown to have antidepressant activity (Chaki et al. 2004) and pro-cognitive effects (Higgins et al. 2004).

LY341495-induced c-Fos response was markedly decreased in the CeM and the LSV in mGlu3-KO mice compared to WT and mGlu2-KO mice, indicating that c-Fos expression is mainly mediated via postsynaptic or glial mGlu3 in these areas. On the other hand, our data indicate a contribution of both group II mGlus to neuronal activation in the LPB. Conversely, in most brain areas, the effect of LY341495 is likely to require a complex and extensive cross talk between the two group II mGlu subtypes in mediating neuronal activation.

**Acknowledgements** Supported by the FWF-NFN-S10202 (to N.S) and FWF-NFN-S10207 (to F.F.)



## References

Anwyl R (1999) Metabotropic glutamate receptors: electrophysiological properties and role in plasticity. Brain Res Brain Res Rev 29:83–120

Beck CH, Fibiger HC (1995) Conditioned fear-induced changes in behavior and in the expression of the immediate early gene c-fos: with and without diazepam pretreatment. J Neurosci 15:709–720

Cartmell J, Schoepp DD (2000) Regulation of neurotransmitter release by metabotropic glutamate receptors. J Neurochem 75:889–907

Chaki S, Yoshikawa R, Hirota S, Shimazaki T, Maeda M, Kawashima N, Yoshimizu T, Yasuhara A, Sakagami K, Okuyama S, Nakanishi S, Nakazato A (2004) MGS0039: a potent and selective group II metabotropic glutamate receptor antagonist with antidepressant-like activity. Neuropharmacology 46(4):457–467

Charney DS, Grillon C, Bremner JD (1998) The neurobiological basis of anxiety and fear: Circuits, mechanisms, and neurochemical interactions (part I). Neuroscientist 4:35–44

Cohen BM, Cherkerzian S, Ma J, Ye N, Wager C, Lange N (2003) Cells in midline thalamus, central amygdala, and nucleus accumbens responding specifically to antipsychotic drugs. Psychopharmacology (Berl) 167:403–410

Conn PJ, Pin JP (1997) Pharmacology and functions of metabotropic glutamate receptors. Annu Rev Pharmacol Toxicol 37:205–237

Corti C, Restituito S, Rimland JM, Brabet I, Corsi M, Pin JP, Ferraguti F (1998) Cloning and characterization of alternative mRNA forms for the rat metabotropic glutamate receptors mGluR7 and mGluR8. Eur J Neurosci 10:3629–3641

Corti C, Aldegheri L, Somogyi P, Ferraguti F (2002) Distribution and synaptic localisation of the metabotropic glutamate receptor 4 (mGluR4) in the rodent CNS. Neuroscience 110:403–420

Corti C, Battaglia G, Molinaro G, Riozzi B, Pittaluga A, Corsi M, Mugnaini M, Nicoletti F, Bruno V (2007) The use of knock-out mice unravels distinct roles for mGlu2 and mGlu3 metabotropic glutamate receptors in mechanisms of neurodegeneration/neuroprotection. J Neurosci 27:8297–8308

Dunayevich E, Erickson J, Levine L, Landbloom R, Schoepp DD, Tollefson GD (2008) Efficacy and tolerability of an mGlu2/3 agonist in the treatment of generalized anxiety disorder. Neuropsychopharmacology 33:1603–1610

Ferraguti F, Shigemoto R (2006) Metabotropic glutamate receptors. Cell Tissue Res 326:483–504

Ferraguti F, Corti C, Valerio E, Mion S, Xuereb J (2001) Activated astrocytes in areas of kainate-induced neuronal injury upregulate the expression of the metabotropic glutamate receptors 2/3 and 5. Exp Brain Res 137:1–11

Franklin KBJ, Paxinos G (1997) The mouse brain in stereotaxic coordinates. Academic, San Diego

Galici R, Jones CK, Hemstapat K, Nong Y, Echemendia NG, Williams LC, de Paulis T, Conn PJ (2006) Biphenyl-indanone A, a positive allosteric modulator of the metabotropic glutamate receptor subtype 2, has antipsychotic- and anxiolytic-like effects in mice. J Pharmacol Exp Ther 318:173–185

Goosens KA, Maren S (2001) Contextual and auditory fear conditioning are mediated by the lateral, basal, and central amygdaloid nuclei in rats. Learn Mem 8:148–155

Helton DR, Tizzano JP, Monn JA, Schoepp DD, Kallman MJ (1998) Anxiolytic and side-effect profile of LY354740: a potent, highly selective, orally active agonist for group II metabotropic glutamate receptors. J Pharmacol Exp Ther 284:651–660

Higgins GA, Ballard TM, Kew JN, Richards JG, Kemp JA, Adam G, Woltering T, Nakanishi S, Mutel V (2004) Pharmacological manipulation of mGlu2 receptors influences cognitive performance in the rodent. Neuropharmacology 46(7):907–917

Hitzemann B, Hitzemann R (1999) Chlordiazepoxide-induced expression of c-Fos in the central extended amygdala and other brain regions of the C57BL/6J and DBA/2J inbred mouse strains: relationships to mechanisms of ethanol action. Alcohol Clin Exp Res 23:1158–1172

Hoffman GE, Lyo D (2002) Anatomical markers of activity in neuroendocrine systems: are we all 'fos-ed out'? J Neuroendocrinol 14:259–268

Johnson MP, Barda D, Britton TC, Emkey R, Hornback WJ, Jagdmann GE, McKinzie DL, Nisenbaum ES, Tizzano JP, Schoepp DD (2005) Metabotropic glutamate 2 receptor potentiators: receptor modulation, frequency-dependent synaptic activity, and efficacy in preclinical anxiety and psychosis model(s). Psychopharmacology (Berl) 179:271–283

Kalin NH, Shelton SE, Davidson RJ (2004) The role of the central nucleus of the amygdala in mediating fear and anxiety in the primate. J Neurosci 24:5506–5515

Kalynchuk LE, Pinel JP, Treit D, Kippin TE (1997) Changes in emotional behavior produced by long-term amygdala kindling in rats. Biol Psychiatry 41:438–451

Kingston AE, Ornstein PL, Wright RA, Johnson BG, Mayne NG, Burnett JP, Belagaje R, Wu S, Schoepp DD (1998) LY341495 is a nanomolar potent and selective antagonist of group II metabotropic glutamate receptors. Neuropharmacology 37:1–12

Kinsey SG, Bailey MT, Sheridan JF, Padgett DA, Avitsur R (2007) Repeated social defeat causes increased anxiety-like behavior and alters splenocyte function in C57BL/6 and CD-1 mice. Brain Behav Immun 21:458–466

Linden AM, Greene SJ, Bergeron M, Schoepp DD (2004) Anxiolytic activity of the MGLU2/3 receptor agonist LY354740 on the elevated plus maze is associated with the suppression of stress-induced c-Fos in the hippocampus and increases in c-Fos

induction in several other stress-sensitive brain regions. Neuropsychopharmacology 29:502–513

Linden AM, Bergeron M, Schoepp DD (2005a) Comparison of c-Fos induction in the brain by the mGlu2/3 receptor antagonist LY341495 and agonist LY354740: Evidence for widespread endogenous tone at brain mGlu2/3 receptors in vivo. Neuropharmacology 49(Suppl):120–134

Linden AM, Shannon H, Baez M, Yu JL, Koester A, Schoepp DD (2005b) Anxiolytic-like activity of the mGLU2/3 receptor agonist LY354740 in the elevated plus maze test is disrupted in metabotropic glutamate receptor 2 and 3 knock-out mice. Psychopharmacology (Berl) 179:284–291

Menard J, Treit D (1996) Lateral and medial septal lesions reduce anxiety in the plus-maze and probe-burying tests. Physiol Behav 60:845–853

Moller C, Wiklund L, Sommer W, Thorsell A, Heilig M (1997) Decreased experimental anxiety and voluntary ethanol consumption in rats following central but not basolateral amygdala lesions. Brain Res 760:94–101

Monn JA, Valli MJ, Massey SM, Wright RA, Salhoff CR, Johnson BG, Howe T, Alt CA, Rhodes GA, Robey RL, Griffey KR, Tizzano JP, Kallman MJ, Helton DR, Schoepp DD (1997) Design, synthesis, and pharmacological characterization of (+)-2-aminobicyclo[3.1.0]hexane-2,6-dicarboxylic acid (LY354740): a potent, selective, and orally active group 2 metabotropic glutamate receptor agonist possessing anticonvulsant and anxiolytic properties. J Med Chem 40:528–537

Muly EC, Mania I, Guo JD, Rainnie DG (2007) Group II metabotropic glutamate receptors in anxiety circuitry: correspondence of physiological response and subcellular distribution. J Comp Neurol 505:682–700

Mutel V, Adam G, Chaboz S, Kemp JA, Klingelschmidt A, Messer J, Wichmann J, Woltering T, Richards JG (1998) Characterization of (2S,2′R,3′R)-2-(2′,3′-[3H]-dicarboxycyclopropyl)glycine binding in rat brain. J Neurochem 71:2558–2564

Oakes ME, Coover GD (1997) Effects of small amygdala lesions on fear, but not aggression, in the rat. Physiol Behav 61:45–55

Ohishi H, Shigemoto R, Nakanishi S, Mizuno N (1993a) Distribution of the messenger RNA for a metabotropic glutamate receptor, mGluR2, in the central nervous system of the rat. Neuroscience 53:1009–1018

Ohishi H, Shigemoto R, Nakanishi S, Mizuno N (1993b) Distribution of the mRNA for a metabotropic glutamate receptor (mGluR3) in the rat brain: an in situ hybridization study. J Comp Neurol 335:252–266

Ornstein PL, Arnold MB, Bleisch TJ, Wright RA, Wheeler WJ, Schoepp DD (1998) [3H]LY341495, a highly potent, selective and novel radioligand for labeling Group II metabotropic glutamate receptors. Bioorg Med Chem Lett 8:1919–1922

Palucha A, Pilc A (2007) Metabotropic glutamate receptor ligands as possible anxiolytic and antidepressant drugs. Pharmacol Ther 115:116–147

Patil ST, Zhang L, Martenyi F, Lowe SL, Jackson KA, Andreev BV, Avedisova AS, Bardenstein LM, Gurovich IY, Morozova MA, Mosolov SN, Neznanov NG, Reznik AM, Smulevich AB, Tochilov VA, Johnson BG, Monn JA, Schoepp DD (2007) Activation of mGlu2/3 receptors as a new approach to treat schizophrenia: a randomized Phase 2 clinical trial. Nat Med 13:1102–1107

Petralia RS, Wang YX, Niedzielski AS, Wenthold RJ (1996) The metabotropic glutamate receptors, mGluR2 and mGluR3, show unique postsynaptic, presynaptic and glial localizations. Neuroscience 71:949–976

Roozendaal B, Koolhaas JM, Bohus B (1991) Central amygdala lesions affect behavioral and autonomic balance during stress in rats. Physiol Behav 50:777–781

Schaffhauser H, Cartmell J, Jakob-Rotne R, Mutel V (1997) Pharmacological characterization of metabotropic glutamate receptors linked to the inhibition of adenylate cyclase activity in rat striatal slices. Neuropharmacology 36:933–940

Schaffhauser H, Richards JG, Cartmell J, Chaboz S, Kemp JA, Klingelschmidt A, Messer J, Stadler H, Woltering T, Mutel V (1998) In vitro binding characteristics of a new selective group II metabotropic glutamate receptor radioligand. Mol Pharmacol 53:228–233 Notes: LY354740, in rat brain

Schoepp DD (2001) Unveiling the functions of presynaptic metabotropic glutamate receptors in the central nervous system. J Pharmacol Exp Ther 299:12–20

Schoepp DD, Johnson BG, Wright RA, Salhoff CR, Monn JA (1998) Potent, stereoselective, and brain region selective modulation of second messengers in the rat brain by (+)LY354740, a novel group II metabotropic glutamate receptor agonist. Naunyn Schmiedebergs Arch Pharmacol 358:175–180

Schoepp DD, Jane DE, Monn JA (1999) Pharmacological agents acting at subtypes of metabotropic glutamate receptors. Neuropharmacology 38:1431–1476

Singewald N, Salchner P, Sharp T (2003) Induction of c-Fos expression in specific areas of the fear circuitry in rat forebrain by anxiogenic drugs. Biol Psychiatry 53:275–283

Spooren WP, Schoeffter P, Gasparini F, Kuhn R, Gentsch C (2002) Pharmacological and endocrinological characterisation of stress-induced hyperthermia in singly housed mice using classical and candidate anxiolytics (LY314582, MPEP and NKP608). Eur J Pharmacol 435:161–170

Tamaru Y, Nomura S, Mizuno N, Shigemoto R (2001) Distribution of metabotropic glutamate receptor mGluR3 in the mouse CNS: differential location relative to pre- and postsynaptic sites. Neuroscience 106:481–503

Tanabe Y, Nomura A, Masu M, Shigemoto R, Mizuno N, Nakanishi S (1993) Signal transduction, pharmacological properties, and expression patterns of two rat metabotropic glutamate receptors, mGluR3 and mGluR4. J Neurosci 13:1372–1378

Wright RA, Arnold MB, Wheeler WJ, Ornstein PL, Schoepp DD (2000) Binding of (2*S*,1′*S*,2′*S*)-2-(9-xanthylmethyl)-2-(2′-carboxycyclopropyl) glycine ([3H]LY341495) to cell membranes expressing recombinant human group III metabotropic glutamate receptor subtypes. Naunyn Schmiedebergs Arch Pharmacol 362:546–554

Wright RA, Arnold MB, Wheeler WJ, Ornstein PL, Schoepp DD (2001) [3H]LY341495 binding to group II metabotropic glutamate receptors in rat brain. J Pharmacol Exp Ther 298:453–460

Yang M, Augustsson H, Markham CM, Hubbard DT, Webster D, Wall PM, Blanchard RJ, Blanchard DC (2004) The rat exposure test: a model of mouse defensive behaviors. Physiol Behav 81:465–473

Yokoi M, Kobayashi K, Manabe T, Takahashi T, Sakaguchi I, Katsuura G, Shigemoto R, Ohishi H, Nomura S, Nakamura K, Nakao K, Katsuki M, Nakanishi S (1996) Impairment of hippocampal mossy fiber LTD in mice lacking mGluR2. Science 273:645–647